Bulgarian Chemical Communications, Volume 52, Special Issue F (pp. 25-31) 2020 DOI: 10.34049/bcc.52.F.0004

Computer modeling of plate heat exchanger for heat utilization from exhaust gases of drying process

P. O. Kapustenko[1], L. L. Tovazhnyanskyy[1], O. P. Arsenyeva[2], S. K. Kusakov[3], V. V. Zorenko[3], O. Y. Fedorenko[1]

[1]*National Technical University, Kharkiv Polytechnic Institute, Dept. ITPA, CRMGET, Kharkiv, Ukraine*
[2] *O. M. Beketov Kharkiv National University, Kharkiv, Ukraine*
[3]*AO Spivdruzhnist-T LLC, Kharkiv, Ukraine*

Received: August 02, 2020 Accepted: August 10, 2020

Based on the mathematical model published in a previous paper for the models of PHE channels corrugated field, a mathematical model of the thermal and hydraulic performance of PHE assembled from commercially produced plates is developed. It accounts for processes at the main corrugated field and also in PHE collectors and channels distribution zones. The results of mathematical modeling are compared with data obtained on a pilot unit for utilization of waste heat from gases coming after tobacco drying. The PHE type TS-6MFG produced by AlfaLaval is tested. The content of the air in the coming air-steam mixture was 10 % at a temperature of 140 °C. The comparison of modeling results and tests data showed good accuracy of prediction. It allowed recommending the obtained correlations and developed mathematical model for the design of plate heat exchangers in applications with heat utilization from exhaust gases after drying processes in the industry.

Keywords: Plate heat exchanger, condensation, noncondensing gas, heat and mass transfer, mathematical model, pressure loss.

INTRODUCTION

Many process technologies require cooling of the gaseous streams, which involves phase change when the working fluids are cooled to the temperatures below the saturation point. It exceeds the heat load of the heat transfer equipment as the latent heat of condensable components is also involved. The process of gaseous stream cooling can be single phase, a process of one component condensation or a process of gaseous mixture condensation, containing condensable and non-condensable components. The presence of condensable vapor in the gas can increase the efficiency of the process, namely in boilers it can lead to 10-12 % raise of condensation of flue gas [1], in ventilation systems it ensures an increased amount of recovered heat [2]. On the other side of the concentration range the content of 0.5 % of non-condensable gas (NCG) in water vapor can lead to a decrease of heat transfer coefficient down to 50% [3]. The vapor condensation from its mixture was studied by many researchers and revealed its importance for refrigeration systems [4], CO_2 and H_2O separation [5], utilisation of heat from flue gases [6] and exhaust gases of combustion engines [7] and others.

The present requirements for higher energy efficiency stipulated the application of more advanced compact heat exchangers with enhanced heat transfer for heat recuperation.

A plate heat exchanger (PHE) corresponds to these requirements in a number of industrial applications. Its construction and operation are sufficiently well described in the literature [8]. PHE has a number of advantages over conventional shell-and-tube heat exchangers. It has smaller size and inventory volume, lower cost, lower fouling, flexible design, access for mechanical surface cleaning, and small temperature approach of streams, down to 1 °C. The heat transfer enhancement allows them to have a smaller heat transfer surface area for the same working conditions. Such features render economically favorable solutions in a number of applications in industry, as, e.g. in CO_2 post-combustion capture plants [9], for heat utilization from exhaust gases [10].

The correct selection of a PHE for specific duty necessitates accounting of all factors influencing its performance, including the construction features of a heat exchanger. The PHE consists of corrugated plates, which as assembled in a pack are forming channels of intricate geometry (see Fig. 1) that promote high levels of turbulence in flows of heat exchanging streams stipulating heat and mass transfer enhancement.

For the accurate design of the PHE used for the condensation of vapor from its mixture with a noncondensing gas, all important factors affecting its performance should be accounted for.

* To whom all correspondence should be sent:
E-mail: sodrut@gmail.com

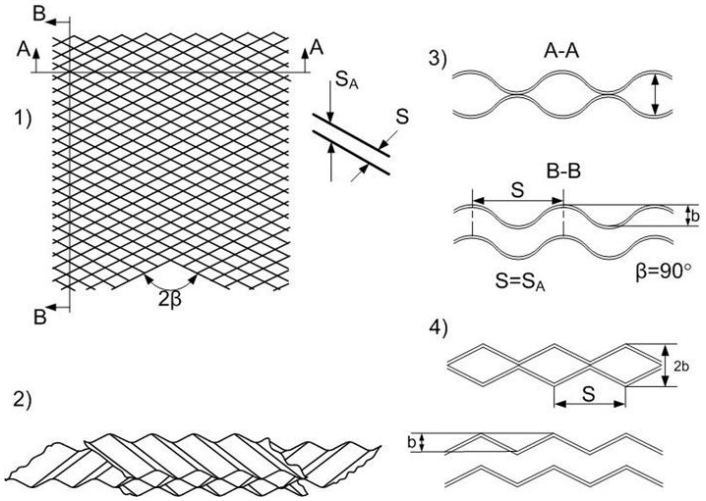

Fig. 1. Scheme of PHE channel corrugated field with various form of plates corrugations: 1, 2 – two neighbor plates intersection; 3 – channels cross-section with sinusoidal corrugations; 4 – channels cross-section with triangular corrugations.

The study of condensation processes in pipes [3] showed that the physical properties of gas and vapor, their concentrations, as well as the geometry of channels and process behavior along the heat transfer surface influence the process intensity. The design of PHEs for cooling a gaseous mixture needs the estimation of heat and mass transfer coefficients and pressure losses in channels, what consists of the following calculations: (1) film heat transfer coefficients at the cooling side, (2) thermal resistance in the condensate film, (3) mass and heat transfer in the vapor-gas mixture and (4) pressure losses in a two-phase flow of gases and liquid.

To calculate the film heat transfer coefficients at the cooling side and the thermal resistance in a condensate film, heat and mass transfer in the condensing flow, the pressure loss in a two-phase flow, the single-phase correlations are needed. The studies of heat transfer and pressure drop in complex criss-cross channels of PHEs are still under investigation and are reported, e.g. for specific plate types [11], or generalized correlations for different corrugations geometries [12], influence of different plate zones on pressure losses in channels for commercial plates [13, 14].

To calculate the heat transfer coefficient in the condensate film, the relations for pure vapor condensation are used. The condensation mechanism is clearly described in [15]. A study of steam condensing in PHE channels is presented in [16]. A review of researches on condensation in PHE channels is given in [17]. For shear driven condensate film flow, the equation based on a homogeneous-dispersed model in the main flow and condensate film flow on the walls is proposed in [18]. The process of heat and mass transport in the gas phase can be estimated by the correlations for the single-phase applying the heat and mass transfer analogy, as analyzed in [19]. Its experimental validation for a small mass flux is reported in [20].

The estimation of pressure losses in a two-phase flow is crucial for the design of PHEs used for condensation. The designed value of pressure drop in PHE unit determines the condensation process in the channels by interacting the driving forces of heat and mass transfer along the plate length due to the vapor equilibrium. Some empirical correlations for condensation for the range of experimental conditions regarding pressure loss for the whole channel length are given in [21]. In [22] the map of different flow regimes for a two-phase flow in PHE channels is presented. The accuracy of pressure loss estimation in a -phase flow depends on how the model corresponds to the experimental conditions.

The state-of-the-art research analysis shows the gap between the data available in literature for laboratory researches and modeling of heat and mass transfer and hydraulic resistance during condensation of gas-vapor mixtures and their validation in industrial conditions, especially for PHE channels of intricated geometry.

In the present paper, a mathematical model proposed in [23] for the models of criss-cross channels is further developed for the thermal design of PHE with commercial plates used for the condensation process. It gives the possibility to determine the process parameters along the channel length and to confirm the accuracy of correlations for pressure losses. The case study of tobacco drying process with application of PHE for condensation of exhaust gases for waste heat utilization is presented.

Model of PHE for Condensation of Gas-Vapor Mixture

The mathematical model of a PHE for condensation based on experimental data, presented in [24] was further improved for the use with commercially produced plates. The main difference of commercially produced plates for PHEs from considered experimental models consists in the design features for flow distribution along the channel and between them. The streams are coming into the PHE *via* connections and are distributed between the channels by collectors organized in the assembled PHE by an arrangement of gaskets around portholes of plates, the flow is distributed from portholes to the main corrugated field by distribution zones as shown in Fig. 2. In the proposed model, the maldistribution of flow between the channels is not accounted for, and the flow rates in all channels are assumed as equal.

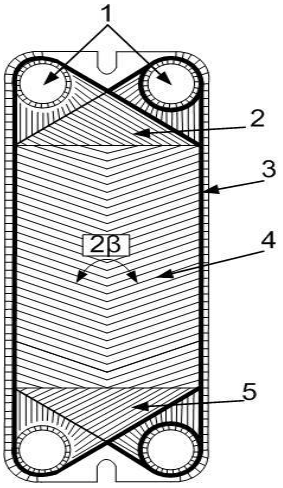

Fig. 2. Schematic drawing of a PHE plate: 1 – heat carrier inlet and outlet; 2,5 – zones for flow distribution; 3 – rubber gasket; 4 –main corrugated field.

It is assumed that the heat and mass transfer processes in all PHE channels are described by correlations and equations determined for the main corrugated field of the channels area. Therefore, the mathematical model presented in paper [24] for criss-cross flow channels with specific geometry is valid also for a PHE with commercial plates having the same corrugation geometry. Another feature difference is the introduction of a more accurate method accounting for the influence on mass transfer of transverse mass flux presented in paper [23] as follows:

The parameter Ψ_D is introduced as the correction factor:

$$\beta_D = \left(D_D / d_e\right) \cdot \Psi_D \cdot Sh_0 \qquad (1)$$

Here D_D is the mass diffusivity m^2/s; β_D is the mass transfer coefficient, m/s; Sh_0 is the Sherwood number calculated by heat and mass transfer analogy:

$$Sh_0 = \frac{\beta_{D0} \cdot \mathrm{d_e}}{D_D} = 0.065 \cdot \mathrm{Re}^{6/7} \cdot \left(\psi \cdot \zeta / F_\mathrm{X}\right)^{3/7} \cdot Sc^{0.4} \qquad (2)$$

where $Sc = \mu/(\rho \cdot D_D)$ is the Schmidt number; F_x is area enlargement factor; Re is the Reynolds number calculated with the channel equivalent diameter.

For accounting the effect of transverse mass flux and the variation of air-stream mixture density from flow core to liquid film surface, the correction coefficient is calculated according to the following equation:

$$\Psi_D = \frac{\ln\left(1+B_m\right)}{B_m} \cdot 4 \cdot \left(1+\sqrt{\frac{\rho_{mx}}{\rho_{mx-f}}}\right)^{-2} \qquad (3)$$

where ρ_{mx} and $\rho_{mx\text{-}f}$ are the densities of the gas-vapor mixture at the main flow and at condensate film surface, respectively, kg/m^3; B_m is mass transfer driving force:

$$B_m = \frac{m_v - m_{v-f}}{m_{v-f} - 1} \qquad (4)$$

Here m_v and $m_{v\text{-}f}$ are mass fractions of vapor in the flow core and on the surface of the liquid film.

The calculations of pressure during the gas-vapor condensation process at the channels main corrugated field is performed with the mathematical model described in [23] that is validated for the experimental models of PHE channel corrugated field as follows.

The total pressure loss in two-phase flow P_{mx} (the first term is for friction losses, the second term is for the acceleration due to change of velocity, and the third term is for geometrical elevation):

$$\frac{dP_{mx}}{dx} = \frac{dP_{TP}}{dx} - \frac{d}{dx}\left(\frac{\rho_{mx} \cdot W_{mx}^2}{2}\right) - \frac{d}{dx}\left(\frac{\rho_{mx} \cdot g \cdot x}{2}\right) \qquad (5)$$

where ρ_{mx} is density of gaseous mixture, kg/m^3; W_{mx} is flow velocity of gaseous mixture, m/s; x is longitudinal coordinate, m; g is gravity force, m^2/s; P_{mx} is the pressure of condensing flow, Pa; dP_{TP}/dx is pressure loss due to friction (including form drug) in two-phase flow, Pa.

For calculation of the pressure losses in condensing two phase flow at PHE channel the combination of two approaches was used. The first one for separate flow of phases is based on Lockhart-Martinelli parameters in the following form:

$$X_{LM} = \sqrt{\frac{dP_L \cdot \phi_L}{dP_G \cdot \phi_G}}; \quad \Phi_G = \sqrt{\frac{dP_{TP}}{dP_G}}; \quad \Phi_L = \sqrt{\frac{dP_{TP}}{dP_L}}; \qquad (6)$$

Here dP_L and dP_G are pressure losses of liquid and gas flowing alone in the channel calculated by correlation for single-phase flow, Pa:

$$dP = \frac{1}{2}\varsigma \cdot \rho \cdot W^2 \cdot \frac{dx}{d_e} \quad (7)$$

where W is the velocity of single-phase flow in a channel, m/s; d_e is channel equivalent diameter, m; ς is friction factor coefficient; ϕ_L and ϕ_G are the share of friction losses in total pressure losses for liquid and gas flowing in channel alone, respectively.

The second approach for pressure loss calculation is based on dispersed-annular flow model and the correlation proposed in the paper by Boyko and Kruzhilin for two phase condensing flow in tubes [25]:

$$dP_{TP} = dP_{0L} \cdot \left[1 + x_{TP} \cdot \left(\frac{\rho_L}{\rho_{mx}} - 1\right)\right] \quad (8)$$

Here dP_{0L} is pressure loss in single-phase flow of liquid determined on a total flow rate of two-phase flow, Pa; ρ_L is density of liquid, kg/m^3; x_{TP} is gas phase mass share in two-phase mixture.

As the application of these approaches separately for all channel length give significantly different and not accurate results for varied types of corrugation, in [23] the improved correlation was proposed, which can account both models of flow structure.

For the channel parts close to the entrance of gas-vapor mixture, where Reynolds numbers calculated for liquid only flowing in channel $Re_L \leq 125$ the following Equation is applied:

$$\Phi_G^2 = 1 + 255 \cdot X_{LM} + X_{LM}^2 \quad (9)$$

For all other channels equation (10) combining both approaches and also accounting for the influence of surface tension forces is used:

$$dP_{TP} = dP_L \cdot \sqrt{1 + x_{TP} \cdot \left(\frac{\rho_L}{\rho_{mx}} - 1\right)} \cdot \left(1 + \frac{7.3 \cdot We^{-0.24}}{X_{LM}} + \frac{0.03}{X_{LM}^2}\right) \quad (10)$$

Here the Weber number is determined as:

$$We = \frac{\rho_{mx} \cdot W_{mx}^2 \cdot d_e}{\sigma} \quad (11)$$

where σ is the surface tension of the liquid, N/m.

The driving forces of heat and mass transfer processes during the condensation of a gas-vapor mixture are influenced by the pressure of the condensing stream due to the pressure effect on vapor partial pressure and saturation temperature. The thermal design of a PHE should take into account the change of pressure at the inlet parts of the PHE and inter-plate channels. The pressure losses at collector inlet, the inlet port and inlet distribution zones can be calculated according to the approach given in [14] for a single-phase flow in a PHE. Here the assumption that the friction pressure loss in a single-phase flow is the same at ports and collectors at the inlet and at the outlet is taken. The recovery of pressure due to the difference of velocities in the collector and in channels must also be considered. When coming to the PHE, where the gas-vapor mixture contains no liquid phase, the pressure loss at the entrance can be calculated as for a single-phase flow. Then the change of pressure at the PHE channel entrance, before the gas-vapor mixture is entering the main corrugated field is calculated according to:

$$\Delta P_{mx.in} = \zeta_{DZin} \cdot \frac{\rho_{mx.in} \cdot W_{mx.in}^2}{2} + 0.65 \cdot \frac{\rho_{mx.in} \cdot W_{pc.in}^2}{2} + \frac{\rho_{mx.in}}{2} \cdot \left(W_{mx.in}^2 - W_{pc.in}^2\right) \quad (12)$$

where $W_{pc.in}$ is the velocity of flow in entrance ports, m/s; $W_{mx.in}$ is the velocity of the gas-vapor mixture at the entrance of the main corrugated field, m/s; $\rho_{mx.in}$ is the density of the incoming gas-vapor mixture, kg/m^3.

For accounting the local pressure losses, the pressure at the entrance to the main corrugated field $P_{mx.cf1}$ is determined by subtraction of pressure drop at the channel entrance from pressure $P_{mx.in}$ at the PHE inlet:

$$P_{mx.cf1} = P_{mx.in} - \Delta P_{mx.in} \quad (13)$$

The total pressure drop in the PHE also includes the pressure loss in the exit distribution zone, port and collector. These pressure drops are determined as local hydraulic resistances calculated on the condensed liquid velocity with a correction factor $(dP_{TP}/dP_L)_{out}$, calculated for the closest to the exit section of a channel as follows:

$$\Delta P_{mx.out} = \left(\zeta_{DZout} \cdot \frac{\rho_{L.out} \cdot W_{L.out}^2}{2} + 0.65 \cdot \frac{\rho_{L.out} \cdot W_{Lpc.out}^2}{2}\right) \times \left(\frac{dP_{TP}}{dP_L}\right)_{out} \quad (14)$$

In eq. (14) $W_{L.out}$ is the velocity calculated for a liquid phase moving alone at the channel exit, m/s; $W_{Lpc.out}$ is the velocity calculated for a liquid phase moving alone in channel exit port, m/s; $\rho_{L.out}$ is the density of outgoing liquid phase, kg/m^3.

The values of the coefficients of local hydraulic resistance at inlet and outlet distribution zones, ς_{DZin} and ς_{DZout} are taken equal to 38, in accordance with data from [14] for a single-phase flow in a PHE with commercial plates. The total pressure drop of a condensing gas-vapor mixture in a PHE by accounting for velocity change at the channel exit is:

$$\Delta P_{mx.PHE} = \Delta P_{mx.in} + \int_0^{L_{pl}} \left(\frac{dP_{TP}}{dx}\right) \cdot dx + \Delta P_{mx.out} + \frac{\rho_{mx.out}}{2} \cdot \left(W_{pc.out}^2 - W_{mx.out}^2\right) \quad (15)$$

where $W_{mx.out}$ is gas-vapor mixture velocity at the channel exit, m/s; $W_{Lpc.out}$ is gas-vapor mixture

velocity in channel exit port, m/s; $\rho_{mx.out}$ is the density of the outgoing gas-vapor mixture, kg/m^3; x is the distance from gas-vapor mixture entrance to channel, m.

For the thermal design of a PHE, mathematical modeling of heat and mass transfer is performed by the equations of the one-dimensional mathematical model proposed in [23]. The heat and mass transfer correlations are taken according to geometrical parameters of corrugations on the main corrugated field with heat transfer area of one plate equal to its total heat transfer area. The calculations were performed for the PHE installed in the industry as is reported in the following case study to check the model validity.

Industrial PHE Test

The use of a PHE for utilization of waste heat from exhaust gases after the drying process at an operating tobacco factory was reported in [10]. At the existing drying plant crushed raw tobacco with a moisture content of about 22.5 % is fed to a drying tunnel, to which superheated steam at a temperature of 180 °C is supplied. In this tunnel, the water inside the tobacco particles boils up, increasing the volume of the particle and partly evaporates to the mainstream. After being kept in the tunnel for about 6–7 s the tobacco particles are separated by precipitation in the cyclone. Tobacco is discharged from the cyclone with a rotary discharger leaving it with 14.5 % moisture content. The remaining steam-air mixture is circulating in the drying circuit, passing through a heat exchanger to maintain the required temperature.

Part of the steam-air mixture containing part of injected steam and steam evaporated from tobacco is discharged into the atmosphere through the adjusting valve. The flow rate of the outgoing part of the steam-air mixture varies from 0.264 to 0.306 kg/s, and its temperature is 140 ºC. It is about 15–19 % of the circulating stream. These exhaust gases are used to heat up an ethylene glycol solution circulating in the heating system of factory workshops and administrative building. PHE AlfaLaval production type TS6M-FG is used for this purpose. The parameters of the PHE and its plates are presented in Table 1.

The measurements of process parameters at the inlet and outlet of the tested PHE were performed during the operation of the drying unit. The results of measurements for four test runs are presented in Table 2. The results of process modeling with the presented mathematical model are also given. The calculations were performed for the measured values of stream flow rates and their parameters at the inlet of the PHE. The calculated outlet temperatures and pressures of the steam-air mixture are also presented in Table 2.

The calculated distribution of process parameters along the length of the PHE channel is presented in Fig. 3 for the conditions of test #2. At the sections of the channel close to the inlet of the steam-air mixture, up to about 0.25 of the relative channel length (x/L_{pl}), there is a steep decrease of gaseous mixture temperature. In this zone, the steam-air mixture is overheated above its saturation temperature.

The cooling of the gaseous mixture in this zone is happening mostly by convection heat transfer from the flow bulk to the channel wall with some condensation at the wall, which temperature is lower than the steam saturation temperature. After the saturation temperature is reached the rate of temperature change decreases and after the equilibrium conditions, it increases again towards the channel exit with increasing air content in the mixture.

Table 1. Main characteristics of the tested PHE TS6M-FG

Parameter	Value
Total number of plates N	50
Heat transfer area of PHE F_{PHE}, m^2	4.80
Heat transfer area of one plate F_{pl}, m^2	0.0850
Channel cross section area, m^2	0.001080
Plate length L_{pl}, m	0.270
Plate width W_{pl}, m	0.276
Area enlargement factor F_X, m/m	1.140
Corrugation pitch S, mm	14.0
Corrugation height b, mm	3.90
Corrugation angle to plate vertical axis β, degrees	60

Table 2. Process parameters

Process parameter	Test #1	Test #2	Test #3	Test #4
Steam-air: flow rate, kg/s	0.2640	0.2780	0.2920	0.3060
inlet temperature, °C	140.0	140.0	140.0	140.0
inlet pressure, Pa	132,000	132,000	131,000	130,000
outlet temperature (measured), °C	76.1	79.1	79.6	81.5
outlet temperature (calculated), °C	75.7	77.9	80.1	82.08
error in outlet temperature), °C	-0.4	-1.2	+0.5	+0.58
pressure drop (measured), Pa	10.10	10.40	12.00	14.40
pressure drop (calculated), Pa	10.21	11.19	12.32	13.51
error in pressure drop, %	+1.1	+7.6	+2.7	-6.2
Cooling media: flow rate, kg/s	7.80	7.80	7.80	7.80
inlet temperature, °C	50.0	50.0	50.0	50.0
outlet temperature (measured), °C	68.0	69.0	69.3	69.5
outlet temperature (calculated), °C	67.41	68.21	68.91	69.61
Total heat load: measured, W	75,23	79,41	80,64	81,50
calculated, W	72,710	76,07	78,97	81,92
Error in heat load, %	-3.3	-4.2	-2.1	+0.5

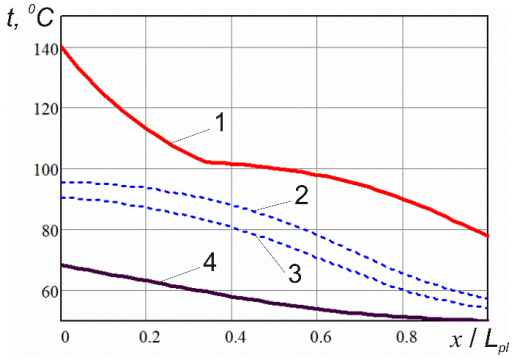

Fig. 3. Distribution of temperatures t along PHE channels relative distance from the entrance of gas-vapor mixture (x/L_{pl}) in test #2: 1 – steam-air mixture; 2 – condensate film surface; 3 – wall; 4 – cooling media

The calculated temperature at the channel exit is lower than its measured value by 1.2 °C; in the other three test runs (see Table 2) this difference is not higher than this value. The difference between the calculated and experimental values of the heat load is less than 4.2 %. This accuracy of thermal modeling of steam-air mixture condensation in the PHE assembled with commercially manufactured plates. The accuracy of predicting the pressure drop is also not exceeding 7.6 %. It is acceptable for practical engineering applications.

CONCLUSIONS

The mathematical model of a PHE accounting for the pressure losses in commercially produced plates is developed and approved for the condensation process using the steam-air gaseous mixture with steam partial condensation as a working fluid. The model validation was performed for the design of the commercially produced PHE installed for heat utilization from exhaust gases coming after the process of tobacco drying at an operating factory. The analysis of modeling results revealed a considerable change of process parameters along the length of PHE channels starting with the cooling of the superheated gaseous mixture at about 1/3 of the PHE surface followed by condensation of steam from a saturated mixture. The developed mathematical model can be used for the design of PHEs in the processes of waste heat utilization from the gaseous stream in different industrial applications and widen the use of PHEs in such conditions

REFERENCES

1. H. Satyavada, S. Baldi, *Energy*, **142**: 121 (2018).
2. S. Gendebien, S. Bertagnolio, V. Lemort, *Energy and Buildings*, **62,** 176 (2013).
3. J. Huang, J. Zhang, L. Wang, *Applied Thermal Engineering*, **89,** 469 (2015).

4. A. Charef, et al., *Heat and Mass Transfer*, **54**(4), 1085 (2018).
5. M. Ge, et al., *Experimental Thermal and Fluid Science*, **75,** 147 *(*2016).
6. I. Zeynali Famileh, J. Abolfazli Esfahani, *International Journal of Heat and Mass Transfer*, **108,** 1466 (2017).
7. K. K. Srinivasan, P. J. Mago, S. R. Krishnan, *Energy*, **35**(6), 2387 (2010).
8. J.J. Klemes, et al., Compact Heat Exchangers for Energy Transfer Intensification: Low Grade Heat and Fouling Mitigation, CRC Press, 2015, p.3 54.
9. O.Y. Perevertaylenko, et al., Energy, vol. page (2015).
10. O.P. Arsenyeva, et al., *Frontiers of Chemical Science and Engineering*, **10**(1), 131 (2016).
11. B. Kumar, A. Soni, S. N. Singh, *Experimental Thermal and Fluid Science*, **91,** 126 (2018).
12. P. Kapustenko, O. Arsenyeva, O. Dolgonosova. in *PRES'11: 14th Conference on Process Integration*, Modelling and Optimisation for Energy Saving and Pollution Reduction, Firenze, Italy, Chemical Engineering Transactions, 2011.
13. S. Gusew, R. Stuke, *International Journal of Chemical Engineering*, **2019**, 3693657 (2019).
14. O. Arsenyeva, et al., *Energy*, **57,** 201 (2013).
15. V.P. Carey, Liquid-Vapor Phase-Change Phenomena: An Introduction to the Thermophysics of Vaporization and Condensation Processes in Heat Transfer Equipment, Third edn., CRC Press, 2020:
16. S. Hu, X. Ma, W. Zhou, *Applied Thermal Engineering*, **113,** 1047 (2017).
17. R. Eldeeb, V. Aute, R. Radermacher, *International Journal of Refrigeration*, **65,** 12 (2016).
18. L. Tovazhnyansky, et al., *Applied Thermal Engineering*, **31**(13), 2146 (2011).
19. W. Ambrosini, et al., *Nuclear Engineering and Design*, **236**(9), 1013 (2006).
20. K. S. Kulkarni, et al., *International Journal of Heat and Mass Transfer*, **113**, 84 (2017).
21. S. B. Al-Shammari, D. R. Webb, P. Heggs, *Desalination*, **169**(2), 151 (2004).
22. X. Tao, M. P. Nuijten, C. A. Infante Ferreira, *International Journal of Refrigeration*, **85,** 489 (2018).
23. P. O. Kapustenko, et al., *Energy*, **201,** 117661 (2020).
24. L. Tovazhnyanskyy, et al., *Bulg. Chem. Commun.*, **50,** 76 (2018).
25. L. D. Boyko, G. N. Kruzhilin, *International Journal of Heat and Mass Transfer*, **10**(3), 361 (1967).